Limnol. Oceanogr., 57(4), 2012, 945–958

doi:10.4319/lo.2012.57.4.0945

Resuspension by fish facilitates the transport and redistribution of coastal sediments

Timor Katz,[a,f,*] Gitai Yahel,[b,c] Matt Reidenbach,[d] Verena Tunnicliffe,[c,e] Barak Herut,[f] John Crusius,[g] Frank Whitney,[h] Paul V. R. Snelgrove,[i] and Boaz Lazar[a]

[a] Institute of Earth Sciences, The Hebrew University of Jerusalem and The Interuniversity Institute for Marine Sciences, Eilat, Israel
[b] The School of Marine Sciences, Ruppin Academic Center, Michmoret, Israel
[c] Department of Biology, University of Victoria, Victoria, British Columbia, Canada
[d] Department of Environmental Sciences, University of Virginia, Charlottesville, Virginia
[e] Victoria Experimental Network Under the Sea (VENUS), University of Victoria, Victoria, British Columbia, Canada
[f] Israel Oceanographic & Limnological Research, Haifa, Israel
[g] U.S. Geological Survey, Woods Hole, Massachusetts
[h] Institute of Ocean Sciences, Sidney, British Columbia, Canada
[i] Ocean Sciences Centre and Biology Department, Memorial University of Newfoundland, St. John's, Newfoundland, Canada

Abstract

Oxygen availability restricts groundfish to the oxygenated, shallow margins of Saanich Inlet, an intermittently anoxic fjord in British Columbia, Canada. New and previously reported ^{210}Pb measurements in sediment cores compared with flux data from sediment traps indicate major focusing of sediments from the oxygenated margins to the anoxic basin seafloor. We present environmental and experimental evidence that groundfish activity in the margins is the major contributor to this focusing. Fine particles resuspended by groundfish are advected offshore by weak bottom currents, eventually settling in the anoxic basin. Transmittance and sediment trap data from the water column show that this transport process maintains an intermediate nepheloid layer (INL) in the center of the Inlet. This INL is located above the redox interface and is unrelated to water density shifts in the water column. We propose that this INL is shaped by the distribution of groundfish (as resuspension sources) along the slope and hence by oxygen availability to these fish. We support this conclusion with a conceptual model of the resuspension and offshore transport of sediment. This fish-induced transport mechanism for sediments is likely to enhance organic matter decomposition in oxygenated sediments and its sequestration in anoxic seafloors.

Sediment focusing occurs where sediments eroded in one location are transport laterally and accumulate at another location. This phenomenon occurs in many areas in the ocean (Dezileau et al. 2000) but most commonly along steep topographic relief (Sugai 1990; Isla et al. 2004). Sediment focusing may greatly affect the dispersal and sequestration of organic matter (Inthorn et al. 2006) and interpretation of the sedimentary record (Pondaven et al. 2000; Francois et al. 2004).

To date, most studies attribute sediment focusing entirely to physical forces such as currents (Sayles et al. 2001; Isla et al. 2004), surface waves (Mullenbach and Nittrouer 2000), and internal waves (Hosegood et al. 2004) or to slumping and seismic events (Dallimore et al. 2005). However, significant and continuous sediment focusing also occurs in calm, deep marine environments where physical processes are weak or infrequent (Sugai 1990; Hales et al. 2006). Lateral transport and dispersion of marine sediments require the initial resuspension of surface sediments, which is not necessarily caused by physical forces. Instead, in many marine habitats, the activity of organisms such as fish (Yahel et al. 2002, 2008), marine mammals (Nelson et al. 1987), and benthic invertebrates (Colin et al. 1986) controls sediment resuspension. Recently, we showed that the activity of groundfish (i.e., fish that live near or at the seafloor) controls sediment resuspension in Saanich Inlet (Yahel et al. 2008), a deep fjord with anoxic bottom water in Vancouver Island, British Columbia, Canada (Fig. 1). Many fish, mostly species of sole, inhabit the oxygenated margins of the inlet seafloor. These flatfish resuspend sediment when preying on near-bottom zooplankton, while digging into the sediment for shelter, or when rising from the sediment to shift location or evade disturbance by other animals. We quantified this fish activity, and concluded that these small fish (~ 10 cm long) rework the surface area of the oxygenated margins once every 2–3 d, resuspending about 1.3 liters bulk sediment m^{-2} d^{-1} (Yahel et al. 2008).

Sediment resuspension also contributes to the formation of nepheloid layers, a term that describes particle-rich and relatively turbid water layers. Nepheloid layers are characterized by enhancement of bacterial activity, organic matter remineralization (Boetius et al. 2000), and chemical scavenging (Bacon and Rutgers Van Der Loeff 1989). When these particle-rich layers form immediately above the seafloor, they are termed benthic nepheloid layers (BNL). BNLs cover vast areas of the ocean floor (McCave 1986). Particle-rich layers found in midwater are termed intermediate nepheloid layers (INLs) and are particularly common over continental margins (McCave 1986). Both types of nepheloid layers also occur in enclosed and semienclosed water bodies such as fjords and lakes.

Published turbidity profiles from different basins suggest dissimilarity between oxygenated and anoxic basins. BNLs

* Corresponding author: timor.katz@mail.huji.ac.il

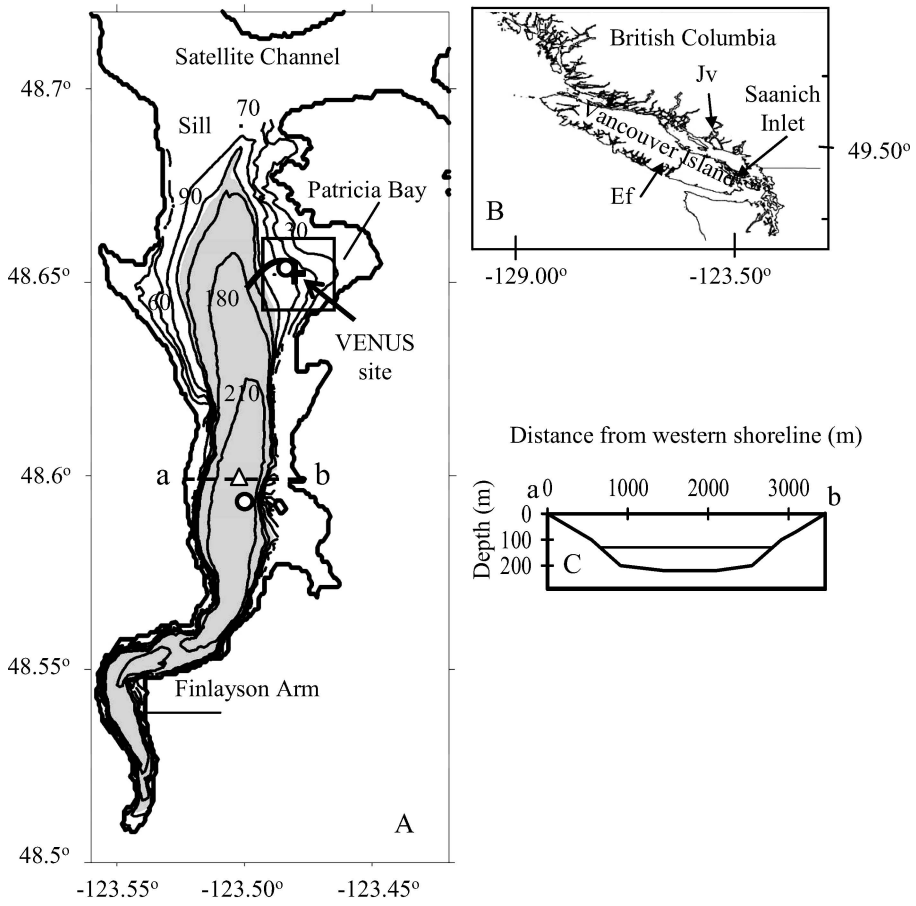

Fig. 1. (A) Bathymetric map of Saanich Inlet. Gray shading marks the area below 130-m depth, which is mostly covered by near-anoxic bottom water and devoid of groundfish. Square frame in Patricia Bay denotes the study area, and black cross mark denotes the location of the dated core. The thick curved line marks the fish survey path. White triangle marks the location of the CTD profiles (Sta. SI5) presented in Fig. 6. Sediment trap arrays are marked by circles; arrow shows the location of the VENUS station. (B) Location of Saanich Inlet in British Columbia. (C) Cross section of the fjord along the a–b line in (A). Jv and Ef in (B) mark the respective locations of Jervis Inlet and Effingham Inlet.

are common in fully oxygenated basins (Pickard and Giovando 1960), whereas anoxic basins are often characterized by narrow INLs frequently situated at the oxic–anoxic interface (Swarzenski et al. 1999; Neretin et al. 2003; Pawlowicz et al. 2007). The formation of these INLs in anoxic basins has been attributed to high abundance of chemosynthetic bacteria (Rozanov et al. 1998; Swarzenski et al. 1999) and, to a lesser degree, to precipitation of Mn and Fe oxides (Neretin et al. 2003). However, De Robertis et al. (2001) and Yahel et al. (2008) showed a different shape of INL in Saanich Inlet fjord in British Columbia, Canada, where turbidity gradually increases from just below the base of the photic zone and starts to decrease near the oxic–anoxic interface. Because turbidity peaks tens of meters above the oxic–anoxic interface, it cannot be explained by redox formation of Mn and Fe precipitates or by the presence of chemosynthetic bacteria therein (Zaikova et al. 2009).

In this study, we examine how resuspension of sediments by groundfish affects sediment focusing and the distribution of suspended matter in the water column of Saanich Inlet. In doing so, we aim to understand better sediment transport in this particular fjord and shed light on a poorly known biophysical mechanism in the sea, with possible implications for organic carbon sequestration and nutrients recycling.

Methods

Study site—Saanich Inlet is a northeast Pacific fjord located at southeastern Vancouver Island, British Columbia (Fig. 1). The inlet reaches maximum depth of 230 m with total surface area of 65 km^2. The inlet is highly productive (mean = 490 g C m^{-2} yr^{-1}; Timothy and Soon 2001) with no major rivers discharging directly into the fjord. Most freshwater input arrives from external rivers. Bottom waters are anoxic most of the year, and this anoxia is reestablished quickly after late summer oxygen renewals as a result of the high productivity and restricted water exchange through the shallow sill (70 m deep) at the mouth of the inlet.

Cowichan River is the nearest major river and discharges into Satellite Channel, north of the inlet sill (Gargett et al.

2003). Particle-rich surface waters entering at the mouth of Saanich Inlet through Satellite Channel (Fig. 1) tend to hug the western shores, creating a gradient in both biogenic and lithogenic particle concentrations from north to south and from west to east (Hobson et al. 2001; Mosher and Moran 2001). Sediment trap measurements at 45–50 m demonstrate a mean annual sediment flux of $\sim$ 1330 g m^{-2} yr^{-1} (Timothy et al. 2003), with much higher values at the mouth (2070 g m^{-2} yr^{-1}) than at the head of the inlet (595 g m^{-2} yr^{-1}). Sediment characteristics are described in detail by Gucluer and Gross (1964) and Blais-Stevens et al. (1997). The sediments in the anoxic basin are mostly laminated, reflecting an annual sedimentation cycle wherein the ratio of plankton (mostly diatoms) to terrestrial matter is higher in the summer and spring and lower in winter (Tunnicliffe 2000). Weak bottom currents suggest minimal physical resuspension over most of the seafloor (Yahel et al. 2008). Storms are rare in the sheltered inlet (*see* Results) and are unlikely to resuspend sediments beyond the shallow perimeter of the inlet. In contrast, biological resuspension at mid-depth in the inlet is extensive. Video recordings and backscatter time series show that groundfish generate about 100 resuspension events m^{-2} d^{-1}, resuspending $\sim$ 1.3 liters bulk (about 1 kg dry) sediment m^{-2} d^{-1} (Yahel et al. 2008; Katz et al. 2009).

Remotely operated vehicle (ROV) survey—We carried out ROV surveys of Saanich Inlet during two cruises onboard the Canadian coastguard ship *J.P. Tully* in July 2005 and February 2006. The Canadian Remotely Operated Platform for Ocean Science (ROPOS; www.ropos.com) ROV was equipped with an online instrument package (Yahel et al. 2008) that included a conductivity, temperature, depth (CTD) sensor package (SBE 19 plus, SeaBird), an oxygen sensor (SBE 43), a transmissometer (25 cm, CStar, WetLabs), and a chlorophyll fluorometer (WETStar, WetLabs). The ROV sampled water characteristics through a 30-cm-long tube positioned atop the ROV, $\sim$ 2 m above bottom (mab). ROPOS was also equipped with video and still cameras, two robotic arms, and corer holders to retrieve sediment cores. The fish study, current measurements, coring, and other ROV work (other than the fish census), were conducted at 80–120-m depth on the eastern slope of Saanich Inlet in Patricia Bay (Fig. 1).

Quantifying fish abundance—We estimated fish abundance along video transects (Fig. 1) from the middle of the inlet (190 m) to Patricia Bay (90 m in July 2005 and 60 m in February 2006). The videos were taken from the ROV as it cruised 1.5 m above the seafloor at an average speed of 14 $\pm$ 10 cm s^{-1} with scaling lasers in every frame (*see* detailed methodology in Yahel et al. 2008). We determined fish distribution based on the x, y, z navigation data from the ROV.

Waves and near-bottom currents—Near-bottom currents and acoustic backscatter (a proxy for suspended sediment concentration) were measured continuously with an acoustic Doppler current meter (2 MHz Aquadopp, Nortek) at the Victoria Experimental Network Under the Sea (VENUS) observatory Saanich site, $\sim$ 1 m above bottom (*see* www.venus.uvic.ca for deployment details). The site is located at the mouth of Patricia Bay (Fig. 1). Data presented here represent an annual cycle from 01 January to 31 December 2010 with the Aquadopp located at 102-m depth (n = 506,579, 1-min averages). We also obtained wave heights measured at a buoy in Patricia Bay between 2001 and 2007 from the Fisheries and Oceans Canada (DFO) Web site (www.meds-sdmm.dfo-mpo.gc.ca/meds/Databases/WAVE/WAVE_e.htm).

Sediment flux (sediment traps)—Sediment flux data were obtained from sediment traps deployed in Saanich Inlet between 1981 and 1983; a description of the methodologies of deployment and sample processing are given in Francois (1988) and Timothy et al. (2003). The traps were deployed in Patricia Bay (48.65°N, 123.49°W; Fig. 1), at a depth of 50 m and at Sta. SI5 (48.59°N, 123.50°W; Fig. 1) at depths of 50, 115, and 180 m.

Near-bottom sediment fluxes were measured with an automated rotating sediment trap that was deployed in Patricia Bay at the VENUS site (48.651°N; 123.486°W) and connected such that operators could open and close the bottles by shore command. The trap (*TECHNICAP* model PPS 4/3-24S) was placed with its opening (0.05-m^2 diameter) 2 m above the oxygenated seafloor at a depth of 94 m. Thirty-six samples were collected intermittently between 2007 and 2009 (sampling intervals 12 h to 19 d). Sediment samples were rinsed with distilled water, freeze-dried, and weighed.

Sedimentation rate—Only one of the cores extracted from the margins of Saanich Inlet was long enough for ^{210}Pb dating. We obtained this core (23 cm long) during February 2006 at a depth of 80 m (48.650°N, 123.476°W) and sectioned it into 1-cm slices. Excess ^{210}Pb was measured by gamma counting (Yang et al. 2007) on a Princeton Gamma-Tech Ge well detector at the laboratories of the U.S. Geological Survey in Woods Hole, Massachusetts.

Water properties measurements—We collected vertical profiles of pressure, temperature, salinity, turbidity (reported as 680-nm light transmittance), chlorophyll fluorescence, and dissolved oxygen concentrations during July 2005 and February 2006 by a SBE-19 plus CTD (SeaBird) mounted on the ROV in dives to the anoxic basin at 48.65°N, 123.5°W; this station was located about 3 km west of the VENUS site. Light transmittance inversely correlates with water turbidity and is determined largely by particle concentrations in the water column (Jones and Wills 1956). Dissolved oxygen data were calibrated using discrete water samples collected by GoFlo bottles and analyzed using computerized Winkler titration as described in Yahel et al. (2008). Additional oceanographic data were obtained from the database of the Institute of Ocean Sciences (IOS), Fisheries and Oceans, Canada. This database contains all available shipboard CTD cast data (as above) from 48.59° N, 123.50° W from 2003 to 2007 and an extensive CTD and light transmittance survey carried by the IOS along west to east

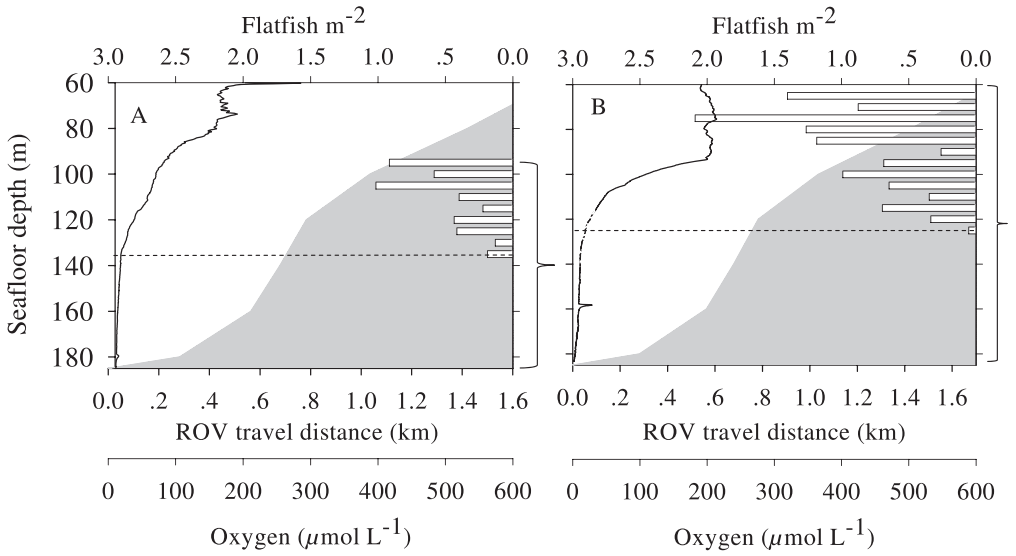

Fig. 2. Fish distribution along the slope of Saanich Inlet from the anoxic basin towards Patricia Bay (see ROV course in Fig. 1) and dissolved oxygen in the water column. (A) July 2005 and (B) February 2006. The seafloor relief is shown as gray shading. White horizontal bars denote abundance of groundfish at or just above the seafloor. Solid lines denote oxygen concentration profiles taken at mid-inlet (start of the survey, ~ 4 km off shore). Broken horizontal lines denote FOB (18 μmol L^{-1}). Inclusion marks to the right of the panels denote the depth range of groundfish surveys.

cross sections of the Inlet (July–November 1995, without oxygen or chlorophyll fluorescence). Additional CTD data from Effingham Inlet, another anoxic fjord in Vancouver Island, were kindly made available to us courtesy of Rick Thomson (IOS).

Fish exclusion experiment—During July 2005 we used the ROV to deploy two cylindrical exclusion cages (excluders) in Saanich Inlet at 92-m depth (*see* study area in Fig. 1) where flatfish were abundant (Katz et al. 2009). The excluders (1-m^2 diameter, 15-cm height with 2.5-cm plastic mesh) prevented fish from reaching the underlying seafloor and reworking the sediment. Two sediment cores were collected at the study area for grain size analysis just before the deployment of the excluders and 7 months later both from inside the excluders and from adjacent, open locations (< 3 m away).

Grain size analysis—Grain size analysis was carried out for the top 4 cm of the sediment in the cores from inside and outside the excluders. Dry sieving (10 min on the shaker) was used to gravimetrically determine the weight fraction of gravel (> 2000 μm) in the surface sediment both from before (July 2005) and from 7 months after cage excluder deployments (February 2006).

Finer grain sizes (0.4–2000 μm) for sediments collected in February 2006 were analyzed using a Beckman Coulter laser diffraction particle size analyzer (*see* methodology in supplementary material for Goodman-Tchernov et al. 2009).

Model—To examine the effect of sediment resuspension along the oxygenated margins on offshore distribution of resuspended fine particles (silt and clay) in Saanich Inlet, we used a simple two-dimensional model based on the Amin and Huthnance (1999) steady-state case. We assume that groundfish activity alone resuspends 1 kg sediment m^{-2} d^{-1} (Katz et al. 2009) and that this activity occurs uniformly along the oxygenated margins down to the depth where oxygen concentrations are too low to support it (~ 130 m; Fig. 2). We then used the model to examine the spatial distribution of sediment in Saanich Inlet, considering realistic cross-slope advection, $u = 0.77$ km d^{-1} (Yahel et al. 2008); vertical eddy diffusivity, $\varepsilon_z = 20 \times 10^{-4}$ m^{-2} s^{-1}, which is in the middle of the range reported for Saanich Inlet (Kunze et al. 2006); and settling velocity (w_s). The settling velocities (w_s) for silt and clay were estimated independently according to Stokes's law using particles and seawater density of 2.6 and 1.025 g cm^{-3}, respectively; viscosity of 0.015 dyne s cm^{-2}; and mean particle diameter of 3 and 20 μm for clay and silt, respectively. Gucluer and Gross (1964) reported that about 11% of the sediments in the margins of Saanich Inlet are silt and clay. Because of the high fall velocity of sand, only clay and silt where considered in the model, and the boundary condition for resuspension rate of silt and clay by fish in the margins was set to 110 g m^{-2} d^{-1}.

Results

Groundfish and dissolved oxygen distribution—Video transects from the deep basin to the margins of Patricia Bay showed a zone devoid of fish that spans the deeper parts of the basin (Fig. 2). Groundfish, mostly slender sole (*Lyopsetta exilis*), appeared while the ROV ascended along the slope to the shallower and oxygenated margins, and their abundance rose steeply within a few tens of meters of depth. We observed additional groundfish species, including flatfish and others, in shallower waters. We frequently observed groundfish resuspending the sediment when

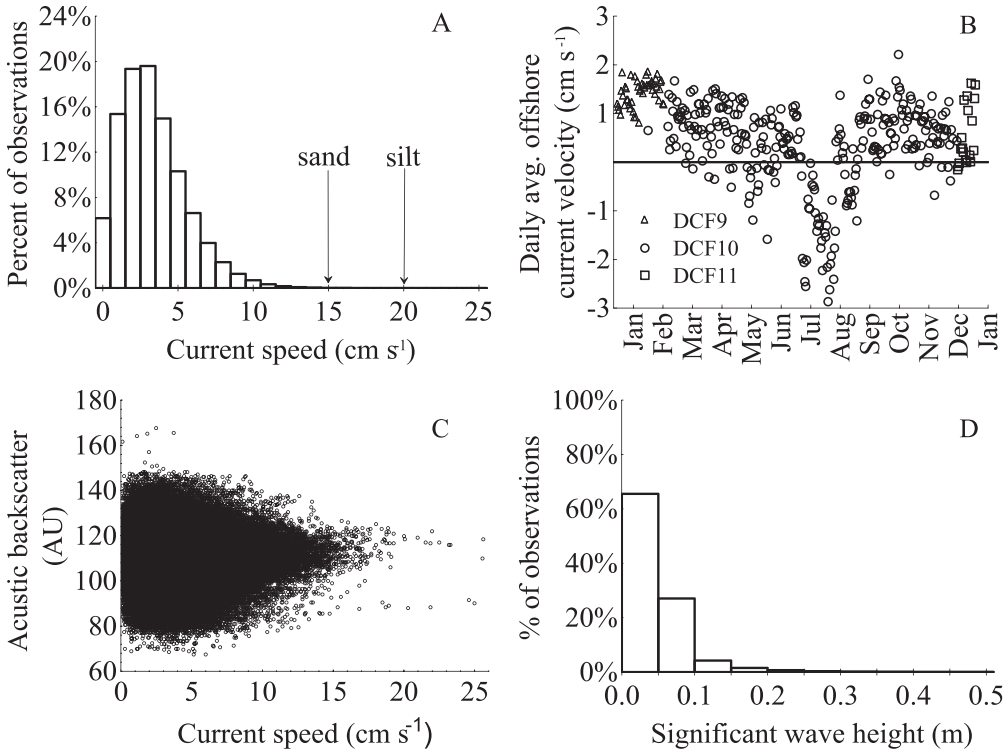

Fig. 3. Summary of near-bottom currents and acoustic backscatter measured with a 2-MHz Aquadopp Current Meter (Nortek) at the VENUS site in Saanich Inlet (between January and December 2010) and wave buoy data between February 2001 and January 2009 from Patricia Bay. (A) Frequency distribution of near-bottom current speed (1-min averages, $n = 506{,}579$); arrows mark resuspension threshold for sand and silt. (B) Daily averages of the offshore (west) component of the near-bottom current velocity; horizontal line marks zero offshore velocity. (C) Acoustic backscatter near the seafloor (as a proxy for suspended particulate matter concentrations) plotted vs. bottom current speeds. A weak negative correlation ($r = -0.02$, $p < 0.001$) indicates that resuspension is not caused by bottom currents. (D) Frequency distribution of significant wave height (m).

digging in, emerging from, or swimming near the seafloor (Yahel et al. 2008). Slender sole tolerance to hypoxia was exceptional, and they occurred at depths where water column dissolved oxygen levels were as low as 18 μmol L^{-1}. However, we found no fish below these concentrations. We therefore termed the depth where we observed 18 μmol O_2 L^{-1} the fish oxygen barrier (FOB). Changing oceanographic conditions shifted the FOB between 135 m in July 2005 and 125 m in February 2006 (Yahel et al. 2008). Note that physiologically, the limiting oxygen concentrations for slender sole are even lower given that concentrations in the benthic boundary layer are likely lower than those measured at similar depth higher in the water column. During these transect surveys, we noted that, while ascending toward the FOB, we crossed from relatively clear water to much more turbid waters; this turbidity at the oxygenated margins persisted thereafter (Yahel et al. 2008).

Near-bottom currents and surface waves—Annual mean ($\pm$ 1 SD) current speed 1 m above the seafloor was 3.5 $\pm$ 2.0 cm s^{-1} in 2007 and 3.8 $\pm$ 2.2 cm s^{-1} in 2010, values considerably lower than the threshold for silt or sand resuspension ($<$ 15 cm s^{-1} at 1 mab; Van Rijn 1993, 2007). In fact, near-bottom currents exceeded 15 cm s^{-1} less than 0.05% of the time (Fig. 3A). The flow direction in Patricia Bay shifted from offshore to onshore every 6–12 h throughout the year but varied in daily predominance of offshore or onshore directions between different seasons (Fig. 3B).

Suspended sediment concentration (measured simultaneously as acoustic backscatter) did not correlate with near-bottom current speed (Fig. 3C), suggesting that currents were not responsible for sediment resuspension at this site. Wave heights measured in Patricia Bay were low throughout the year, with average significant wave height of 10 cm; 99.9% of all waves were < 0.5 m; and high-energy storms were absent from the wave record (Fig. 3D).

Sediment fluxes (sediment traps)—Mean sediment flux measured 2 m above the bottom at 95-m depth in Patricia Bay (VENUS site, 2007 and 2009) was 13.4 g dry sediment m^{-2} d^{-1} ($n = 36$; SD = 7.4). Lacking comparable measurements from the water above, we analyzed unpublished data from sediment trap arrays deployed in the water column during the 1980s. The mean sediment flux in Patricia Bay in sediment traps deployed at 50-m depth in 1983 (Fig. 1) was 3.6 $\pm$ 0.9 g dry sediment m^{-2} d^{-1} ($n = 12$ monthly deployments), about a quarter of the near-bottom flux.

Results from sediment trap arrays in Sta. SI5 over the anoxic basin (Fig. 1) are shown in Table 1. Note that the

Table 1. Total particle fluxes (g dry sediment m^{-2} d^{-1}) at Sta. SI5 in Saanich Inlet (*see* Fig. 1) and the flux ratios between consecutive depths.

Date	Flux at 50 m	Flux at 115 m	Flux at 180 m	$Flux_{115}$: $flux_{50}$	$Flux_{180}$: $flux_{115}$
Dec-81	2.33	3.32	3.36	1.42	1.01
Apr-82	3.34	6.86	5.92	2.05	0.86
Jul-82	1	1.51	1.33	1.51	0.88
Nov-82	2.41	2.35	2.78	0.98	1.18
Feb-83	2.74	3	2.93	1.09	0.98
Mar-83	2.52	5.21	4.49	2.07	0.86
May-83	1.59	4.29	3.39	2.7	0.79
Jun-83	3.17	5.63	4.36	1.78	0.77
Jul-83	1.59	3.22	2.89	2.03	0.9
Aug-83	3.96	5.1	4.06	1.29	0.8
Sep-83	2.56	3.3	2.78	1.29	0.84
Mean (SD)	2.5 (0.9)	4.0 (1.6)	3.5 (1.2)	1.7 (0.5)	0.9 (0.1)

sediment flux increased by a factor of 1.7 between the shallow trap at 50-m depth and the mid-water trap at 115-m depth. This increase with depth in the oxygenated waters occurred in 10 of the 11 sets of measurements ($p < 0.002$; *t*-test for paired samples). In contrast, there was a slight yet significant flux decrease ($p < 0.02$; *t*-test for paired samples) between the mid-water trap, just above the average FOB depth of 121 m ± 16.7, ($n = 22$ CTD casts at Sta. I5), and the deep trap (180 m) in the anoxic waters.

Sedimentation rate—A 12-cm-deep mixed layer in the 23-cm-long core used for dating suggests intense sediment reworking of the upper sediment. Based on a log-linear fit ($R^2 = 0.86$) of the ^{210}Pb profile beneath the mixed layer (Fig. 4A) and the sediment porosity (Fig. 4B), we calculated a sedimentation rate of 0.1 cm yr^{-1} (Appleby 2008). Assuming dry density of 2.7 g cm^{-3}, this sedimentation rate implies a concurrent accumulation rate (*see* Eq. 1 in the Discussion) of 0.5 kg dry sediment m^{-2} yr^{-1} (~ 1.4 g dry sediment m^{-2} d^{-1}).

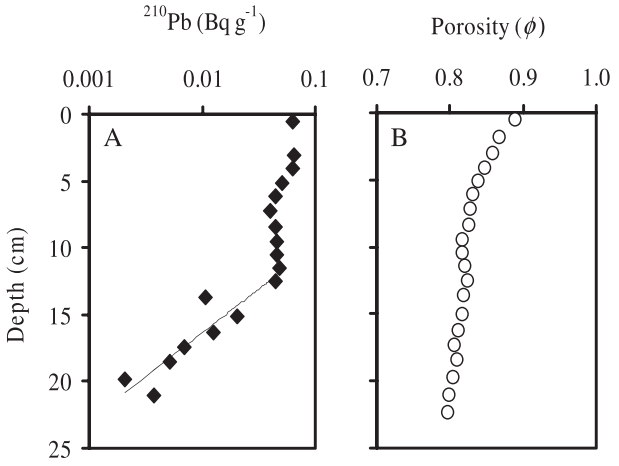

Fig. 4. (A) ^{210}Pb and (B), porosity profiles in the dated sediment core from Patricia Bay (80-m depth). Regression beneath the mixed surface layer suggests sedimentation rate of 0.1 cm yr^{-1}.

Fish exclusion experiment—Seven months after the deployment of the fish excluders, the sediment underneath the excluders differed fundamentally from nearby sediments exposed to unabated fish activity (Fig. 5). Within the fish excluders, we observed a large accumulation of fine silt and clays; mean sediment grain size was 8 μm (range 0.4–53 μm) compared to 61 μm (range 0.4–1300 μm not including gravel) outside the excluders (Fig. 5A). Moreover, gravel (solid stones > 2 mm) occurred in the surface sediments (top 4 cm) at the study site prior to excluder deployment. Seven months after the deployment, such gravel was still present outside the excluders, but none was present in the surface sediments (top 4 cm) inside the excluders (Fig. 5B).

Turbidity and oxygen in the water column—In Saanich Inlet, the anoxia depth (where dissolved O_2 concentrations ≈ 0) and the FOB (18 μmol O_2 L^{-1}) above it shift up and down in response to changing hydrographic conditions. For example, between February 2003 and October 2007, the shallowest anoxia depth in Sta. SI5 was 102 m (results not shown), and the mean anoxia depth was 147 m (Fig. 6A). Intermittent availability of oxygen in deeper waters (Fig. 7) results from the late summer renewal event during which oxygenated, dense Pacific waters spill over the sill and extend along the Inlet bottom (Anderson and Devol 1973). The persistence of a significant INL shallower than the FOB was evident in almost all the vertical profiles from the water column overlying the anoxic basin (Fig. 6A). Below the phytoplankton-rich photic zone (20 m; Timothy and Soon 2001), turbidity greatly decreases but gradually increases from a depth of ~ 50 m downward, forming a turbidity hump just above the FOB (Figs. 6, 7). Deeper than the FOB, at the oxic–anoxic interface (anoxia depth), a second, more condensed turbidity peak often appears (Fig. 6B). Thereafter, turbidity gradually decreases toward the bottom of the anoxic basin. Cross-inlet (east to west) transects conducted in 1995 and during this study reveal a well-developed benthic nepheloid layer over the oxygenated margins of the Inlet (above the FOB; Figs. 8, 9A). These marginal BNLs then extend to the mid-water as INLs (Fig. 8).

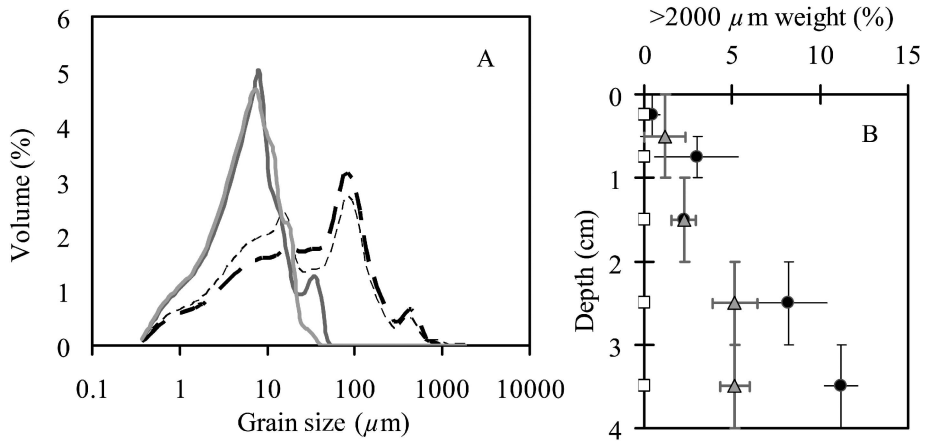

Fig. 5. Grain size analysis in surface sediments (0–4 cm) at the fish excluder cage site. (A) Fine grain size distribution by volume (< 2000 μm; 92 size bins) in sediments collected from inside the excluders (solid lines) and from nearby points outside (dashed lines; < 3 m away); note the logarithmic scale in the x-axis. (B) Profiles of the percent (by weight) of gravel (> 2000 μm) in the sediment sampled in July 2005, prior to deployment of the fish excluders (gray triangles) and from inside (white squares) and outside the excluders (< 3 m away; solid black circles) in February 2006. Horizontal and vertical error bars mark the range between two cores and thickness of the sediment slice, respectively.

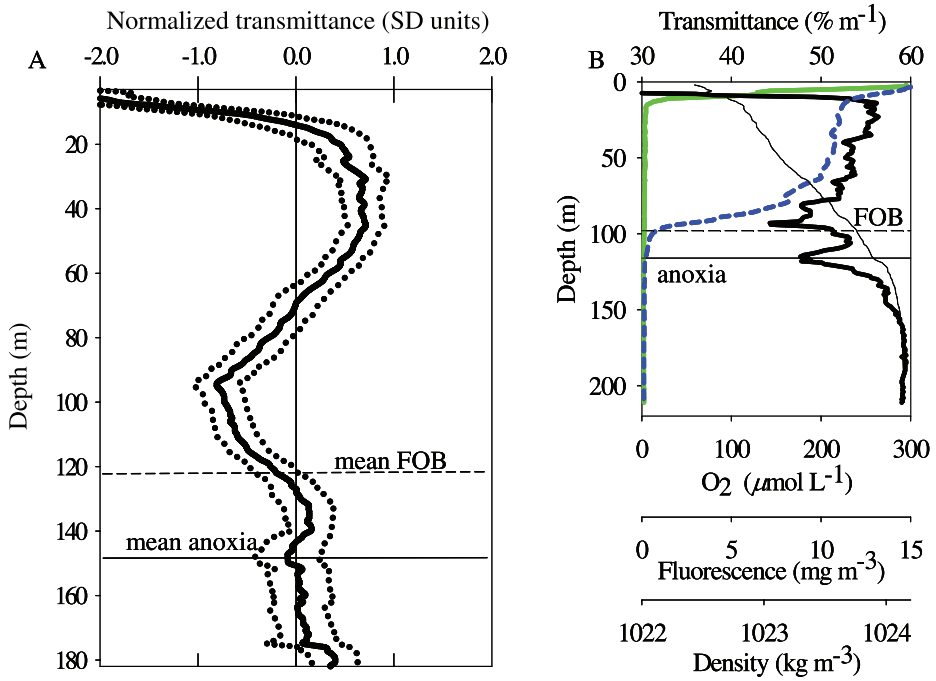

Fig. 6. (A) Normalized light transmittance plot for 41 mid-inlet profiles (2003–2007). Solid line denotes average transmittance. Dotted lines show 95% confidence interval of the mean for each depth interval (1 m). To allow comparison between profiles, each datum ($X_{z,i}$) was normalized to the mean ($\bar{X}_i$) and standard deviation (SD) of the ith profile as norm $Xz,i = (Xz,i - \bar{X}i)/\mathrm{SD}i$ This rescaling to profiles standard deviation units allowed us to pool light transmittance measurements from four annual cycles. Note that where all three lines cross the 0 SD (mean for each profile), the mean light transmittance is significantly different ($p < 0.05$) from the profile mean. Dashed and solid horizontal lines denote the FOB and anoxia depth, respectively. (B) Vertical profiles of light transmittance (inverse of turbidity, thick black), dissolved oxygen concentrations (dashed blue), chlorophyll concentrations (green), and water density (thin black) measured at the mid-inlet sampling station (white triangle in Fig. 1) during May 2005. Dashed and solid horizontal lines denote the FOB and anoxia depth, respectively.

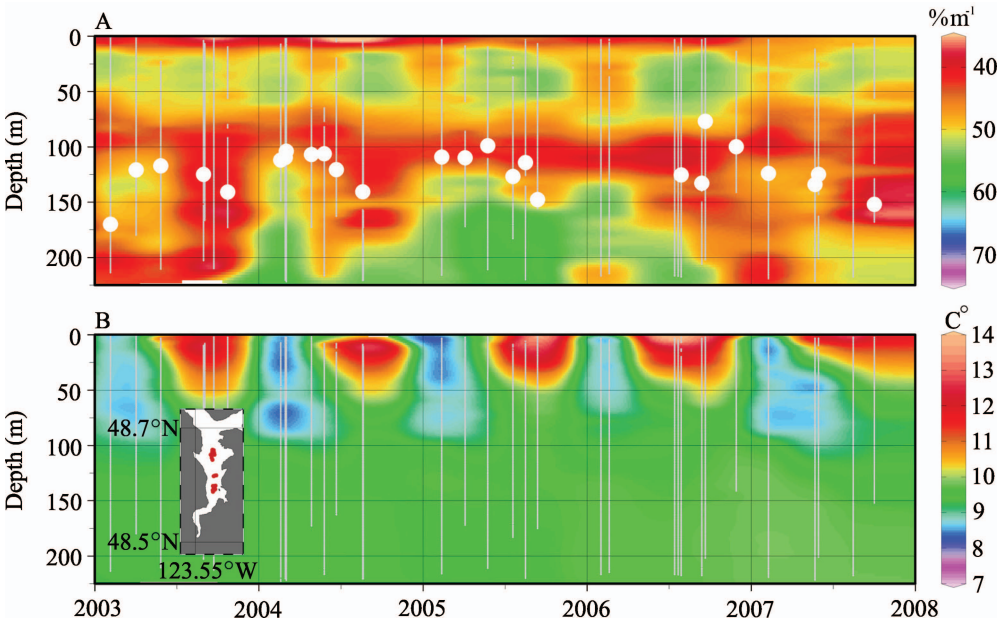

Fig. 7. Time series of (A) turbidity measured as light transmittance (% m^{-1}; color shading) and depth of the FOB ($[O_2]$ = 18 μmol L^{-1}; white dots) and (B) temperature from casts taken at the mid-inlet stations (n = 41) from 2003 to 2007. Red dots denote sampling locations in inset map. Sampling times and depths are shown with vertical gray lines. Note the persistence of the INL. We observed a deep BNL on several occasions. The intermittent occurrence of BNLs appears to be associated with renewal events.

A deep BNL also occurred several times in the anoxic zone. This intermittent occurrence of deep BNLs below the FOB occurs in late summer and is apparently associated with late summer renewal events. We also observed temporal changes in pycnocline depth, but these were unrelated to the depths of the FOB or the INL (*see* example in Fig. 6B).

Model results—As depicted in Fig. 10, the two-dimensional model (Amin and Huthnance 1999) predicts the formation of a BNL over the margins where fish reworked the sediment (shallower than 130 m) and of an offshore maximum of fine particle concentrations (INL) located at or above the FOB when offshore currents prevail (Fig. 10).

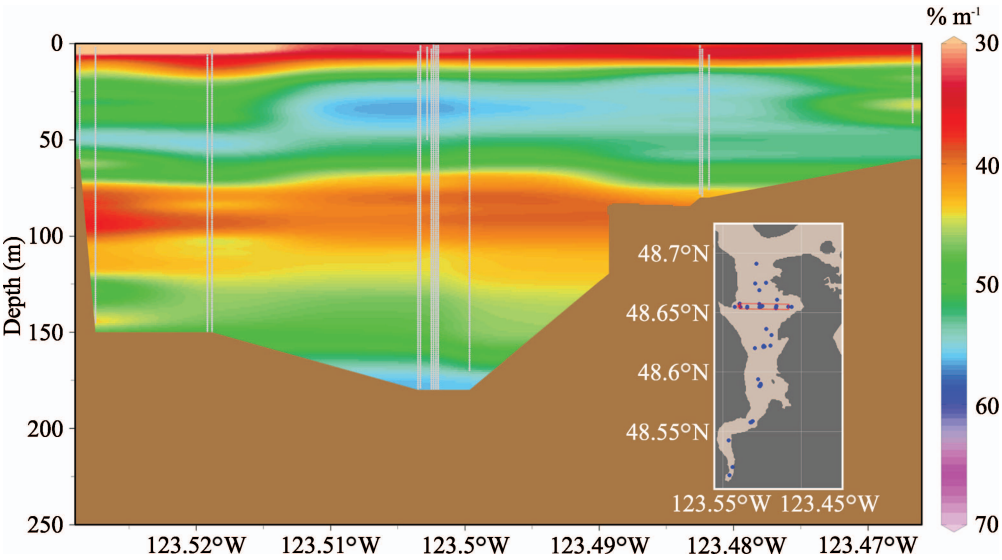

Fig. 8. Transmittance (% m^{-1}) gradient in colors from CTD casts taken during 1995 along east-to-west transects in Saanich Inlet. Sampling locations are shown as vertical gray lines and as blue dots in inset map. Brown shading approximates the bottom based on the logged bottom depths at the sampling locations. The triangular protrusion at the eastern margins is a software artifact caused by missing data and does not reflect actual seafloor topography.

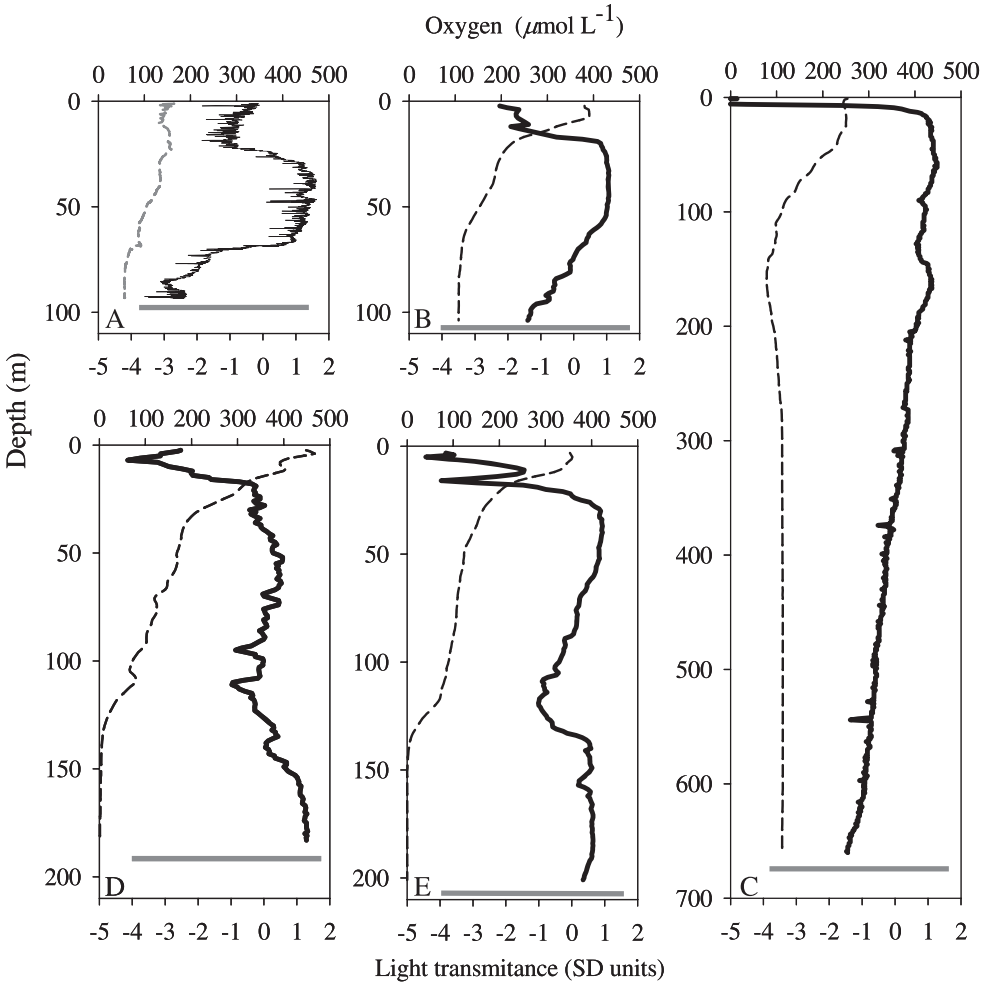

Fig. 9. Dissolved oxygen (dashed) and transmittance profiles (solid) in the water column from three British Columbian fjords. Profiles are shown for (A) oxygenated margins and (D) anoxic basin of Saanich Inlet, (B) oxygenated and (E) anoxic basins in Effingham Inlet (49.05°N, 125.15°W), and (C) the deep oxygenated basin of Jervis Inlet (49.84°N, 123.90°W). The transmittance profiles in all panels were normalized as in Fig. 6A to allow pooling and cross comparison between different instruments, basins, and seasons. Gray horizontal lines at the bottom of each panel denote the seafloor depth.

Discussion

Sediment fluxes measured by near-bottom sediment traps demonstrate intense sediment resuspension in the oxygenated margins of Saanich Inlet. Mean sediment fluxes measured from 2007 to 2009 in Patricia Bay at 2 m above the seafloor (near the VENUS station at 96-m depth) were 13.4 g dry sediment $m^{-2}\,d^{-1}$, almost four times higher than those measured some 40 m above (at 50-m depth) in 1983. Given our observations of the seafloor and weak near-bottom currents and surface waves that are insufficient to resuspend sediment (Fig. 3), we attribute this sediment resuspension at the seafloor to intense groundfish activity (Yahel et al. 2008).

Sediment focusing in Saanich Inlet—Focusing in a sedimentary basin is the transport (lateral redistribution) of settled sediments from the margins to the deep basin. Sediment focusing can be demonstrated by the ratio between the observed accumulation rate (A, kg m^{-2} yr^{-1}) and the expected accumulation rate (A_F) based on the particle flux (rain) reaching the seafloor from surface waters and the degradation rate of particles (e.g., decomposition of organic matter) therein. A net import of sediments into a focusing area yields $A : A_F > 1$, whereas erosion, or net export of sediments at the source of the focusing, where particles first settled yields $A : A_F < 1$.

Matsumoto and Wong (1977) estimated the accumulation rate in Saanich Inlet basin from ^{210}Pb measurements to be 2.7 kg m^{-2} yr^{-1}. We calculated a similar value of 2.5 kg m^{-2} yr^{-1} from the sedimentation rate of 1.3 cm yr^{-1} reported by Blais-Stevens et al. (1997) based on varve thickness:

$$A = 10\omega(1-\phi)\rho \quad (1)$$

where ω is the sedimentation rate in cm yr^{-1}; ϕ denotes sediment porosity (0.92; Murray et al. 1978), ρ is the density of dry basin sediments (2.4 g cm^{-3}; Gucluer and

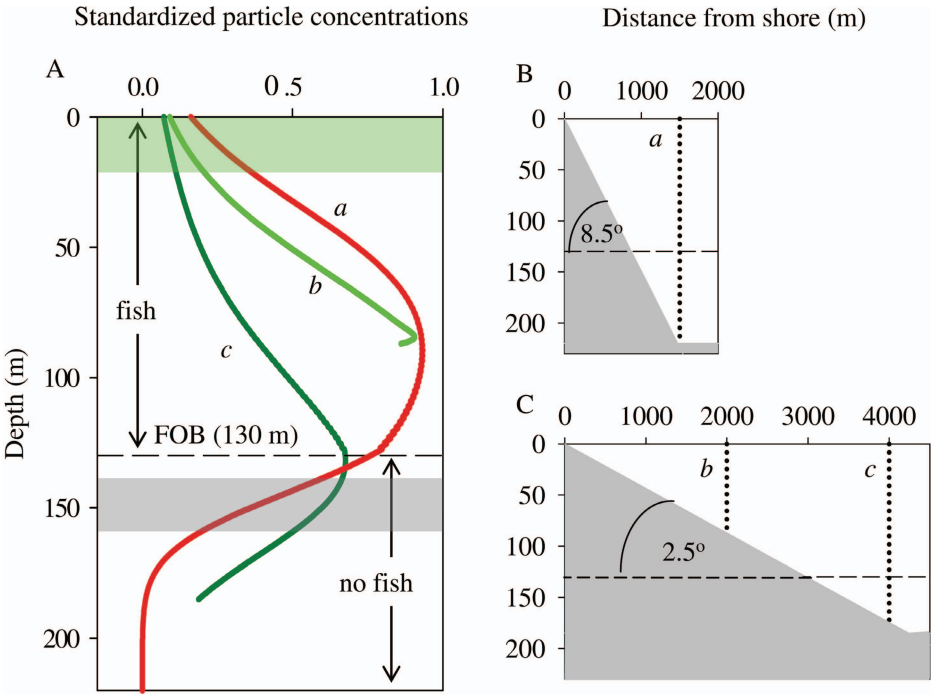

Fig. 10. (A) Model predictions for resuspended particle concentrations, normalized by near-bottom silt and clay concentrations resuspended by fish activity along the margins, assuming mean offshore advection of 0.77 km d^{-1} (mean during 2007), uniform resuspension along the slope to a 130-m-deep FOB (dashed line in all panels), and no resuspension beneath it. Lines *a*, *b*, and *c* mark particle concentration profiles at different slope angles and offshore distances as shown in (B) and (C). Each profile is drawn to the depth where it would intercept the seafloor. (A) Shaded areas mark other sections in the water column where observed turbidity was high, that is, the surface photic layer (0–20 m) where phytoplankton concentrations are high (green) and the anoxia depth (mean 147 m) beneath the FOB (e.g., Fig. 6B) where chemosynthetic and redox processes take place (gray). Margin slopes of (C) 2.5° and (B) 8.5° correspond to the mean slope in Patricia Bay and in section a–b in Fig. 1, respectively.

Gross 1964), and the factor 10 converts units from g cm^{-2} yr^{-1} to kg m^{-2} yr^{-1}. We used this somewhat unconventional unit conversion from grams to kilograms because of the exceptionally high accumulation rate (and sediment flux) in Saanich Inlet.

Sediment fluxes are composed of biogenic (organic matter, calcium carbonates and opal) and lithogenic components (e.g., clay minerals). In Saanich Inlet, the biogenic flux originates from *in situ* and imported surface water productivity (Timothy and Soon 2001) and the lithogenic flux arrives from local runoff and external river freshets (Fraser River and Cowichan River), entering through the mouth of the inlet (Gargett et al. 2003; Timothy et al. 2003). The biogenic flux below the photic zone decreases with depth as a result of decay and dissolution processes (Timothy 2004). However, the flux of refractory lithogenic material is generally preserved during settlement (and mostly thereafter). We therefore assumed that the flux of lithogenic material from the surface water equals the rain of lithogenic material (R_L), and in the absence of lateral transport, the accumulation rate of lithogenic material (A_L) equals its rain; in a high deposition basin such as Saanich Inlet, authigenic processes at the seafloor should be minor and we ignore them hereafter.

We calculated the accumulation rate of refractory lithogenic sediments at the anoxic basin off Patricia Bay to be ~ 1.8 kg m^{-2} yr^{-1} based on the following equation:

$$A_L = A[1 - (f_{POM} + f_{opal} + f_{CaCO3})] \quad (2)$$

where A_L is the accumulation rate of lithogenic material, A is the total sediment accumulation rate (2.6 kg m^{-2} yr^{-1}), and f_{POM}, f_{opal}, and f_{CaCO3} are the weight fractions of particulate organic matter, opal, and $CaCO_3$, respectively. The values of f_{POC} (2.9%), f_{opal} (24%), and f_{CaCO3} (2.4%) were taken from Gucluer and Gross (1964), and f_{POM} was calculated as 1.9 f_{POC} (Timothy et al. 2003).

The mean flux of lithogenic material at 45-m depth, 1.5 km to the north of Patricia Bay, was calculated from the difference between the total sediment flux (2.07 kg m^{-2} yr^{-1}) and the flux of biogenic material in Timothy et al. (2003) to be 1.06 kg m^{-2} yr^{-1}. As discussed above, this flux should equal the flux of lithogenic material reaching the sediment and its expected accumulation therein ($A_{L(F)}$). The $A_L : A_{L(F)}$ ratio for the anoxic basin adjacent to Patricia Bay was therefore estimated to be 1.8, indicating that about half the lithogenic material that accumulates in the basin arrives by lateral transport and not from the surface water. Sediment trap data from Sta. SI5 (Table 1), 10 km to the

south of the sill, corroborate this conclusion, showing that the sediment flux in mid-water (115-m depth) is ~ 1.7 times greater than that at 50-m depth (Table 1). We suggest that this sediment addition arrives at the mid-water trap from resuspension at the margins (*see* turbidity plumes in Fig. 8) where fish rework the seafloor.

The rate of sediments accumulation at the oxygenated seafloor also suggests lateral transport of sediments from the margins. Based on our ^{210}Pb dating, we calculated a sedimentation rate in Patricia Bay of 0.1 cm yr^{-1} equaling the accumulation of ~ 0.5 kg dry sediment m^{-2} yr^{-1} (Eq. 1). Given that about 90% of the sediment in the dated core was lithogenic, the accumulation rate of lithogenic material, A_L should be 0.45 kg m^{-2} yr^{-1}. The mean sediment flux at 50-m depth over Patricia Bay (during 1983) was 1.3 kg m^{-2} yr^{-1}. The mean ratio of organic carbon to dry sediment weight in this trap (6.6%) was close to fluxes reported by Timothy et al. (2003) from nearby Sta. SI9 at the mouth of the inlet (6.2%), where 50% of the flux is lithogenic (*see* above). We therefore assumed a similar ratio of lithogenic to total flux and calculated the rain of lithogenic matter (R_L) over Patricia Bay and its expected accumulation rate ($A_{L(F)}$) to be ~ 0.65 kg m^{-2} yr^{-1}. This estimate suggests that the $A_L : A_{L(F)}$ ratio in the oxygenated margins is only 0.7, indicating seafloor erosion and off-margins export of sediment.

Lateral transport from the western margins to the basin likely exceeds that than from Patricia Bay in the east (Mosher and Moran 2001). There is an inherent difficulty in calculating $A_L : A_{L(F)}$ ratio with sediment traps data since trapping efficiency is often $\neq$ 100% (Yu et al. 2001). This sampling problem should be relatively minor in Saanich Inlet, where currents are slow and the waters calm, but nonetheless adds uncertainty to the calculations. In general, trapping efficiency $<$ 100% implies a smaller $A_L : A_{L(F)}$ ratio that reduces the excess accumulation signal in the basin but increases the seafloor erosion signal in the margins; the opposite is expected for trapping efficiency $>$ 100%.

A biophysical mechanism for sediment focusing in Saanich Inlet—Saanich Inlet sediment is constantly transported from the margins to the deep anoxic basin. Such sediment focusing is often attributed to seismic activity and gravity failures. However, the intact record of annual varves in the anoxic basin in Saanich Inlet during the last 130 yr or more (Tunnicliffe 2000) precludes these factors as major causes for recent sediment focusing. A more plausible mechanism is ongoing advection of resuspended sediments from the margins by offshore currents. At shallow depths, surface waves may cause resuspension (Mullenbach and Nittrouer 2000). In deeper waters, away from regions where surface waves break, sediment resuspension is commonly attributed to shear stress induced by strong bottom currents (Isla et al. 2004) and internal waves (Puig et al. 2001; Hosegood et al. 2004). In Saanich Inlet, small surface waves (Fig. 3) and weak bottom currents (whether caused by seiches, tides, or wind) cannot resuspend sediment ($<$ 15 cm s^{-1} at 1 mab; Van Rijn 1993, 2007); instead, our work suggests that groundfish reworking of the seafloor causes most of the resuspension (Yahel et al. 2008). This finding point to a novel biophysical mechanism that involves chronic biological resuspension along the slope combined with offshore near-bottom currents that together cause seafloor erosion at the margins and lateral transport and focusing of fine (silt and clay) sediments to the deep basin. The big difference between the resuspension rate of silt and clay by fish and their calculated transport from the margins (~ 110 g m^{-2} d^{-1} vs. a few g m^{-2} d^{-1}, respectively), indicates that the vast majority of the resuspended fine particles remain aggregated, quickly falling back to the seafloor.

Focusing and sediment winnowing—Unlike slumping, ongoing resuspension and lateral sediment transport causes sediment winnowing and fining with depth (Wheatcroft and Butman 1997). Indeed, Gucluer and Gross (1964) measured median grain size of 258 μm in the oxygenated margin compared to only 5.9 μm in the anoxic basin.

Our excluder experiment in Saanich Inlet demonstrated the absence of sediment winnowing therein. The excluders prevented groundfish from entering and reworking the seafloor, and within 7 mo, fine silt and clays (mean grain size 8 μm) accumulated inside the excluders to a depth of a few centimeters. The nearby surface sediments outside the excluders were much coarser, containing silts and fine sand (mean grain size 61 μm; Fig. 5A) and gravel. The freshly deposited layer of fine sediments inside the excluders ($>$ 4 cm) buried small gravel fragments that were prevalent in the surface sediments prior to the cage deployment (Fig. 5B). Whereas sediment winnowing and seafloor erosion continued unabated outside the excluders, it was halted and even reversed inside the excluders that became the ultimate recipients of fine sediments that were resuspended around them by the groundfish (Fig. 3; Yahel et al. 2008), comparable to what we propose for the deep basin.

Sediment resuspension and nepheloid layer formation—Sediment resuspension by fish in the margins also affects water column properties. An intermediate nepheloid layer (INL) represents a prominent feature in the turbidity profiles along the central axis of Saanich Inlet above the FOB (Figs. 6, 7). This feature was previously shown but not explained by De Robertis et al. (2001) and Yahel et al. (2008). This mid-depth INL is a statistically significant (Fig. 6A) and persistent feature of the water column overlying the anoxic basin (Fig. 7). The INL mean depth in Saanich Inlet is 99 m $\pm$ 13 m (n = 21 transmissometer casts between 2003 and 2007). In some places, bottom currents (e.g., from internal wave reflection) generate bed shear stress sufficient to resuspend sediment along the margins or shelf break and initiate mid-water INLs along density interfaces (McCave 1986). Aggregation of particles at density interfaces may be common in the ocean, but close examination of the data for Saanich Inlet shows no relationship between the depths of the INL and the pycnocline (e.g., Fig. 6B). Previous work already associated groundfish activity with the formation of BNLs (Yahel et al. 2002, 2008). When such resuspension occurs along a slope, fine resuspended particles can be transported from the slope bottom by offshore currents to form INLs. This mechanism should be particularly conspicuous where fish population aggregate or, as in Saanich Inlet, are limited to a specific depth.

In addition to the mid-water INL, located above the FOB, two other turbidity feature are commonly observed in Saanich Inlet: a high-turbidity zone, which is always associated with the photic zone where phytoplankton concentrations are high (e.g., Fig 6B), and a deep INL, located beneath the FOB (Figs. 6B, 7). This is most likely a redox nepheloid layer (Rosanov et al. 1998; Neratin et al. 2003), which is caused by high concentrations of microbes at the oxic–anoxic interface; such bacteria aggregates were recently shown in Saanich Inlet by Zaikova et al. (2009).

Groundfish distribution along the slope and INLs in the water column—The decrease in dissolved oxygen concentrations in the deeper water of Saanich Inlet creates a depth barrier for fish distribution, the FOB, below which groundfish are absent (Fig. 2). Whereas some fish, most notably the slender sole (*Lyopsetta exilis*), can cope with extremely low dissolved oxygen concentrations, no fish occur in Saanich Inlet below the 18 μmol O_2 L^{-1} depth. Fish abundance starts to decline in hypoxic waters < 65 μmol O_2 L^{-1} (Vaquer-Sunyer and Duarte 2008). In the July 2005 and February 2006 fish surveys, fish abundance started to decline about 30 m above the FOB (Fig. 2). Moreover, the depth of the FOB shifted frequently. For example, the 135-m-deep FOB in July 2005 decreased to 125 m by February 2006 (Fig. 2). Therefore, groundfish in Saanich Inlet must retreat to shallower regions when the depth at which hypoxia occurs rises, and they return to deeper waters only once hypoxia subsides. Pihl et al. (1991) describe similar fish behavior in Chesapeake Bay. In an intermittently anoxic basin such as Saanich Inlet, this groundfish movement would alter the areas of biologically reworked and resuspended seafloor. Such shifts may have basin-scale implication for mineralization and sequestration of organic matter (Yahel et al. 2008) and dissolution of biogenic silica (Katz et al. 2009). Oxygen-driven shifts in groundfish distributions may also affect sediment features, such as annual lamination and thus interpretation of sediment stratigraphy.

By resuspending sediment, groundfish maintain a conspicuous BNL over the oxygenated margins (Yahel et al. 2008; Fig. 9A). Turbidity (low transmittance) plumes originating from these BNLs at the oxygenated margins to the west and east of the inlet extend above the FOB (far above the anoxic interface) toward the mid-basin (Fig. 8). These plumes form an INL with a mid-water turbidity maximum at the center of the inlet (Figs. 7, 8) at a mean depth of 99 m (Fig. 6A). This maximum is approximately 23 m shallower than the mean FOB depth of 122 m (SD = 17 m; $n = 21$ CTD casts) in our 2003–2007 databases. This difference is not trivial. Because the slope of the seafloor dictates that groundfish reworking the sediment close to the FOB are the nearest resuspension sources to the center of the inlet, the turbidity max would be expected to form closer to the FOB depth (*see* model results in Fig. 10).

Two observations explain this divergence: the reduction in groundfish abundance and hence in sediment resuspension below $\sim$ 100-m depth (Fig. 2) and the thick bacterial mats (mostly *Beggiatoa* sp.) that cover the seafloor in this hypoxic depth zone (Juniper and Brinkhurst 1986; Yahel et al. 2008) and limit the disaggregation of fine particles from the resuspended sediments (Holland et al. 1974; Sutherland et al. 1998).

The model results (Fig. 10) further support our biophysical explanation for the INL formation. It shows that offshore advection of resuspended fine sediments at the oxygenated margins will form an INL at or above the FOB. According to our model, no INLs will form during average onshore bottom currents (results not shown). This prediction appears at odds with the persistence of the mid-inlet INL (Figs. 6, 7) because there are documented periods in Patricia Bay when onshore currents prevail (Fig. 3B). However, our model predicts that a mid-inlet INL will form as long as offshore currents persist over either the western or the eastern side of the inlet (*see* turbidity plume off the western margins in Fig. 8). If similar fish activity and an offshore current from the other side of Saanich Inlet balance an onshore current at the opposite side, a constant INL will likely form in the center of the inlet. Note that because the turbidity peaks in the surface water (0–20 m) and beneath the FOB (Fig. 6B) are caused by high concentrations of microorganisms (*see* above), they cannot be considered in our model (Fig. 10).

Where fish rework the seafloor, the model predicts the formation of a benthic nepheloid layer (BNL) regardless of storm occurrence. In basins with anoxic deep waters, this BNL is expected only over the oxygenated margins but not in the anoxic basin. Similarly, in calm, fully oxygenated basins, a BNL should persist at all depths. This prediction matches the transmittance profiles from three calm British Columbian fjords: Saanich Inlet, where the basin is anoxic (Fig. 9D) and the margins oxygenated (Fig. 9A); Effingham Inlet, from both an anoxic basin (Fig. 9E) and an oxygenated basin (Fig. 9B); and Jervis Inlet, a deep and fully oxygenated basin (Fig. 9C; Pickard and Giovando 1960). Available sediment flux data from the oxygenated margins in Patricia Bay (at the surface and near the seafloor) and over the anoxic basin in Sta. SI5 in Saanich Inlet (Table 1) correspond with both the transmittance profiles (Figs. 6, 8) and our model predictions (Fig. 10). These data are also consistent with reported increases in sediment fluxes toward the deep seafloor from sediment trap arrays in fully oxygenated Jervis Inlet (Timothy et al. 2003).

Biophysical sediment focusing in the ocean—Sediment resuspension by groundfish (and other animals) is not unique to Saanich Inlet. Fish that resuspend sediments (e.g., rays: Sasko et al. 2006; goatfish: Yahel et al. 2002; cod: Katz et al. 2009) inhabit most marine environments. However, most studies overlook this phenomenon and its relative importance in explaining redistribution of marine sediments. Although sediment disturbance by fish may be negligible in some marine environments, our data demonstrate that in areas where currents are weak and wave energy is low, fish activity can be the dominant sediment resuspension mechanism facilitating sediment transport and focusing. While potentially more significant for calm water bodies, biophysical sediment transport and focusing by groundfish resuspension complements physical transport and may be important in many aquatic environments from lakes to the deep sea. We suggest that dispersal and

burial rates of organic carbon and other chemical compounds in sediments are regulated in part by biophysical sediment transport wherever large mobile animals interact with sloping seafloor and soft sediments.

Acknowledgments

We thank J. M. Rose and the teams of the Canadian Remotely Operated Platform for Ocean Science (ROPOS), Canadian coastguard ship *J.P. Tully*, and Victoria Experimental Network Under the Sea (VENUS) for their most professional and enthusiastic help during field sampling and sample processing. We are grateful to the Department of Fisheries and Oceans, Canada, for permission to use their oceanographic database from Saanich, Jervis, and Effingham Inlets. We also thank Vera Pospelova and Andrea Price for the sediment trap data and Beverly Goodman and McMaster University for help with grain-size analysis. The VENUS Project and University of Victoria supported the ship and submersible time for field experiments, and the U.S. Geological Survey and Coastal and Marine Geological Program generously supported J.C. The project was supported by Discovery Grants from the Natural Sciences and Engineering Research Council of Canada to V.T. and P.S. and a Yohay Ben-Nun fellowship and Moshe Shilo Center for Marine Biogeochemistry Fund award to T.K.

References

Amin, M., and J. M. Huthnance. 1999. The pattern of cross-slope depositional fluxes. Deep-Sea Res. I **46:** 1565–1591, doi:10.1016/S0967-0637(99)00020-5

Anderson, J. J., and A. H. Devol. 1973. Deep water renewal in Saanich Inlet, an intermittently anoxic basin. Estuar. Coast. Mar. Sci. **1:** 1–10, doi:10.1016/0302-3524(73)90052-2

Appleby, P. G. 2008. Three decades of dating recent sediments by fallout radionuclides: A review. The Holocene **18:** 83–93, doi:10.1177/0959683607085598

Bacon, M. P., and M. M. Rutgers Van Der Loeff. 1989. Removal of thorium-234 by scavenging in the bottom nepheloid layer of the ocean. Earth Planet. Sci. Lett. **92:** 157–164, doi:10.1016/0012-821X(89)90043-5

Blais-Stevens, A., J. J. Clague, P. T. Bobrowsky, and R. T. Patterson. 1997. Late Holocene sedimentation in Saanich Inlet, British Columbia, and its paleoseismic implications. Can. J. Earth Sci. **34:** 1345–1357, doi:10.1139/e17-107

Boetius, A., B. Springer, and C. Petry. 2000. Microbial activity and particulate matter in the benthic nepheloid layer (BNL) of the deep Arabian Sea. Deep-Sea Res. II **47:** 2687–2706, doi:10.1016/S0967-0645(00)00045-X

Colin, P. L., T. H. Suchanek, and G. McMurtry. 1986. Water pumping and particulate resuspension by callianassids (Crustacea: Thalassinidea) at Enewetak and Bikini Atolls, Marshall Islands. Bull. Mar. Sci **38:** 19–24.

Dallimore, A., R. E. Thomson, and M. A. Bertram. 2005. Modern to late Holocene deposition in an anoxic fjord on the west coast of Canada: Implications for regional oceanography, climate and paleoseismic history. Mar. Geol. **219:** 47–69, doi:10.1016/j.margeo.2005.05.003

De Robertis, A., K. Eiane, and G. H. Rau. 2001. Eat and run: Feeding and subsequent aerobic recovery by *Orchomene obtusus* in Saanich Inlet, British Columbia, Canada. Mar. Ecol. Prog. Ser. **219:** 221–227, doi:10.3354/meps219221

Dezileau, L., G. Bareille, J. L. Reyss, and F. Lemoine. 2000. Evidence for strong sediment redistribution by bottom currents along the southeast Indian ridge. Deep-Sea Res. I **47:** 1899–1936, doi:10.1016/S0967-0637(00)00008-X

Francois, R. 1988. A study on the regulation of the concentrations of some trace-metals (Rb, Sr, Zn, Pb, Cu, V, Cr, Ni, Mn And Mo) in Saanich Inlet sediments, British-Columbia, Canada. Mar. Geol. **83:** 285–308, doi:10.1016/0025-3227(88)90063-1

———, M. Frank, M. Van Der Loeff, and M. Bacon. 2004. ^{230}Th normalization: An essential tool for interpreting sedimentary fluxes during the late Quaternary. Paleoceanography **19:** PA1018, doi:10.1029/2003PA000939

Gargett, A. E., D. Stucchi, and F. Whitney. 2003. Physical processes associated with high primary production in Saanich Inlet, British Columbia. Estuar. Coast. Shelf Sci. **56:** 1141–1156, doi:10.1016/S0272-7714(02)00319-0

Goodman-Tchernov, B. N., H. W. Dey, E. G. Reinhardt, F. McCoy, and Y. Mart. 2009. Tsunami waves generated by the Santorini eruption reached Eastern Mediterranean shores. Geology **37:** 943–946, doi:10.1130/G25704A.1

Gucluer, S. M., and G. M. Gross. 1964. Recent marine sediments in Saanich Inlet, a stagnant marine basin. Limnol. Oceanogr. **9:** 359–376, doi:10.4319/lo.1964.9.3.0359

Hales, B., L. Karp-Boss, A. Perlin, and P. A. Wheeler. 2006. Oxygen production and carbon sequestration in an upwelling coastal margin. Glob. Biogeochem. Cycles **20:** GB3001, doi:10.1029/2005GB002517

Hobson, L. A., M. R. McQuoid, and V. Tunnicliffe. 2001. The Saanich Inlet basin: A natural collector of past biological, climatic, and land-use changes in southwestern Canada amplified by results of ODP leg 169S. Geosci. Can. **28:** 197–202.

Holland, A. F., R. G. Zingmark, and J. M. Dean. 1974. Quantitative evidence concerning the stabilization of sediments by marine benthic diatoms. Mar. Biol. **27:** 191–196, doi:10.1007/BF00391943

Hosegood, P., J. Bonnin, and H. Van Haren. 2004. Solibore-induced sediment resuspension in the Faeroe-Shetland Channel. Geophys. Res. Lett. **31:** L09301, doi:10.1029/2004GL019544

Inthorn, M., T. Wagner, G. Scheeder, and M. Zabel. 2006. Lateral transport controls distribution, quality, and burial of organic matter along continental slopes in high-productivity areas. Geology **34:** 205–208, doi:10.1130/G22153.1

Isla, E., P. Masque, A. Palanques, J. Guillen, P. Puig, and J. A. Sanchez-Cabeza. 2004. Sedimentation of biogenic constituents during the last century in western Bransfield and Gerlache Straits, Antarctica: A relation to currents, primary production, and sea floor relief. Mar. Geol. **209:** 265–277, doi:10.1016/j.margeo.2004.06.003

Jones, D., and M. S. Wills. 1956. The attenuation of light in sea and estuarine waters in relation to the concentration of suspended solid matter. J. Mar. Biol. Assoc. U. K. **35:** 431–444, doi:10.1017/S0025315400010250

Juniper, S. K., and R. O. Brinkhurst. 1986. Water-column dark CO_2 fixation and bacterial-mat growth in intermittently anoxic Saanich Inlet, British-Columbia. Mar. Ecol. Prog. Ser. **33:** 41–50, doi:10.3354/meps033041

Katz, T., and others. 2009. Groundfish overfishing, diatom decline, and the marine silica cycle: Lessons from Saanich Inlet, Canada, and the Baltic Sea cod crash. Glob. BiogeochemCycles **23:** GB4032, doi:10.1029/2008GB003416

Kunze, E., J. F. Dower, I. Beveridge, R. Dewey, and K. P. Bartlett. 2006. Observations of biologically generated turbulence in a coastal Inlet. Science **313:** 1768–1770, doi:10.1126/science.1129378

Matsumoto, E., and C. S. Wong. 1977. Heavy metal sedimentation in Saanich Inlet measured with ^{210}Pb technique. J. Geophys. Res. **82:** 5477–5482, doi:10.1029/JC082i034p05477

McCave, I. N. 1986. Local and global aspects of the bottom nepheloid layers in the world ocean. Neth. J. Sea Res. **20:** 167–181, doi:10.1016/0077-7579(86)90040-2

Mosher, D. C., and K. Moran. 2001. Post-glacial evolution of Saanich Inlet, British Columbia: results of physical property and seismic reflection stratigraphic analysis. Mar. Geol. **174:** 59–77, doi:10.1016/S0025-3227(00)00142-0

Mullenbach, B. L., and C. A. Nittrouer. 2000. Rapid deposition of fluvial sediment in the Eel Canyon, northern California. Cont. Shelf Res. **20:** 2191–2212, doi:10.1016/S0278-4343(00)00067-4

Murray, J. W., V. Grundmanis, and W. M. Smethie. 1978. Interstitial water chemistry in sediments of Saanich Inlet. Geochim. Cosmochim. Acta **42:** 1011–1026, doi:10.1016/0016-7037(78)90290-9

Nelson, C. H., K. R. Johnson, and J. H. Barber. 1987. Gray whale and walrus feeding excavation on the Bering Shelf, Alaska. J. Sed. Res. **57:** 419–430.

Neretin, L. N., C. Pohl, G. N. Jost, T. Leipe, and F. Pollehne. 2003. Manganese cycling in the Gotland Deep, Baltic Sea. Mar. Chem. **82:** 125–143, doi:10.1016/S0304-4203(03)00048-3

Pawlowicz, R., S. A. Baldwin, A. Muttray, J. Schmidtova, B. Laval, and G. Lamont. 2007. Physical, chemical, and microbial regimes in an anoxic fjord (Nitinat Lake). Limnol. Oceanogr. **52:** 1002–1017, doi:10.4319/lo.2007.52.3.1002

Pickard, G. L., and L. F. Giovando. 1960. Some observations of turbidity in British Columbia inlets. Limnol. Oceanogr. **5:** 162–170, doi:10.4319/lo.1960.5.2.0162

Pihl, L., S. P. Baden, and R. J. Diaz. 1991. Effects of periodic hypoxia on distribution of demersal fish and crustaceans. Mar. Biol. **108:** 349–360, doi:10.1007/BF01313644

Pondaven, P., O. Ragueneau, P. Treguer, A. Hauvespre, L. Dezileau, and J. L. Reyss. 2000. Resolving the opal paradox in the Southern Ocean. Nature **405:** 168–172, doi:10.1038/35012046

Puig, P., A. Palanques, and J. Guillen. 2001. Near-bottom suspended sediment variability caused by storms and near-inertial internal waves on the Ebro mid continental shelf (NW Mediterranean). Mar. Geol. **178:** 81–93, doi:10.1016/S0025-3227(01)00186-4

Rozanov, A. G., L. N. Neretin, and I. I. Volkov. 1998. Redox nepheloid layer (RNL) of the Black Sea: Its location, composition and origin, p. 77–91. *In* L. I. Ivanov and T. Oguz [eds.], Ecosystem modeling as a management tool for the Black Sea. NATO Science Series 2 Environmental Security.

Sasko, D. E., M. N. Dean, P. J. Motta, and R. E. Hueter. 2006. Prey capture behavior and kinematics of the Atlantic cownose ray, *Rhinoptera bonasus*. Zoology **109:** 171–181, doi:10.1016/j.zool.2005.12.005

Sayles, F. L., W. R. Martin, Z. Chase, and R. F. Anderson. 2001. Benthic remineralization and burial of biogenic SiO_2, $CaCO_3$, organic carbon, and detrital material in the Southern Ocean along a transect at 170° West. Deep-Sea Res. II **48:** 4323–4383, doi:10.1016/S0967-0645(01)00091-1

Sugai, S. F. 1990. Transport and sediment accumulation of Pb-210 and Cs-137 in two southeast Alaskan fjords. Estuaries **13:** 380–392, doi:10.2307/1351783

Sutherland, T. F., C. L. Amos, and J. Grant. 1998. The effect of buoyant biofilms on the erodibility of sublittoral sediments of a temperate microtidal estuary. Limnol. Oceanogr. **43:** 225–235, doi:10.4319/lo.1998.43.2.0225

Swarzenski, P. W., B. A. McKee, J. M. Skei, and J. F. Todd. 1999. Uranium biogeochemistry across the redox transition zone of a permanently stratified fjord: Framvaren, Norway. Mar. Chem. **67:** 181–198, doi:10.1016/S0304-4203(99)00058-4

Timothy, D. A. 2004. Organic matter remineralisation and biogenic silica dissolution in a deep fjord in British Columbia, Canada: A regression analysis of upper ocean sediment-trap fluxes. Deep-Sea Res. I **51:** 439–456, doi:10.1016/j.dsr.2003.10.009

———, and M. Y. S. Soon. 2001. Primary production and deep-water oxygen content of two British Columbian fjords. Mar. Chem. **73:** 37–51, doi:10.1016/S0304-4203(00)00071-2

———, ———, and S. E. Calvert. 2003. Settling fluxes in Saanich and Jervis Inlets, British Columbia, Canada: Sources and seasonal patterns. Prog. Oceanogr. **59:** 31–73, doi:10.1016/j.pocean.2003.07.001

Tunnicliffe, V. 2000. A fine-scale record of 130 years of organic carbon deposition in an anoxic fjord, Saanich Inlet, British Columbia. Limnol. Oceanogr. **45:** 1380–1387, doi:10.4319/lo.2000.45.6.1380

van Rijn, L. C. 1993. Principles of sediment transport in rivers, estuaries and coastal seas. Aqua Publications.

———. 2007. Unified view of sediment transport by currents and waves. II: Suspended transport. J. Hydraul. Eng. **133:** 668–699, doi:10.1061/(ASCE)0733-9429(2007)133:6(668)

Vaquer-Sunyer, R., and C. M. Duarte. 2008. Thresholds of hypoxia for marine biodiversity. Proc. Natl. Acad. Sci. **105:** 15452–15457, doi:10.1073/pnas.0803833105

Wheatcroft, R. A., and C. A. Butman. 1997. Spatial and temporal variability in aggregated grain-size distributions, with implications for sediment dynamics. Cont. Shelf Res. **17:** 367–390, doi:10.1016/S0278-4343(96)00035-0

Yahel, G., R. Yahel, T. Katz, B. Lazar, B. Herut, and V. Tunnicliffe. 2008. Fish activity: A major mechanism for sediment resuspension and organic matter remineralization in coastal marine sediments. Mar. Ecol. Prog. Ser. **372:** 195–209, doi:10.3354/meps07688

Yahel, R., G. Yahel, and A. Genin. 2002. Daily cycles of suspended sand at coral reefs: A biological control. Limnol. Oceanogr. **47:** 1071–1083, doi:10.4319/lo.2002.47.4.1071

Yang, L., X. Li, J. Crusius, U. Jans, M. E. Melcer, and P. Zhang. 2007. Persistent chlordane concentrations in Long Island Sound sediment: Implications from chlordane, ^{210}Pb, and ^{137}Cs profiles. Environ. Sci. Technol. **41:** 7723–7729, doi:10.1021/es070749a

Yu, F., R. Francois, M. Bacon, S. Honjo, A. Fleer, S. Manganini, v. d. Loeff, M. Rutgers, and V. Ittekot. 2001. Trapping efficiency of bottom-tethered sediment traps estimated from the intercepted fluxes of ^{230}Th and ^{231}Pa. Deep-Sea Res. I **48:** 865–886, doi:10.1016/S0967-0637(00)00067-4

Zaikova, E., D. A. Walsh, C. P. Stilwell, W. W. Mohn, P. D. Tortell, and S. J. Hallam. 2009. Microbial community dynamics in a seasonally anoxic fjord: Saanich Inlet, British Columbia. Environ. Microbiol. **12:** 172–191, doi:10.1111/j.1462-2920.2009.02058.x

Associate Editor: Bo Thamdrup

Received: 08 August 2011
Accepted: 22 January 2012
Amended: 28 January 2012